Optical Coherence Propagation and Imaging in a Multiple Scattering Medium

Sajeev John, Gendi Pang, and Yumin Yang
University of Toronto, Department of Physics, Toronto, Ontario, Canada M5S 1A7

Abstract

We present a formal, microscopic, solution of the wave propagation problem for an inhomogeneity embedded in an isotropically disordered, multiple scattering, homogeneous background. The inhomogeneity is described by a local change in the complex, dielectric autocorrelation function $B(\mathbf{r},\mathbf{r}') \equiv \omega^4/c^4 \langle \epsilon^*(\mathbf{r})\epsilon(\mathbf{r}') \rangle_{\text{ensemble}}$ for a wave of frequency w and velocity c. For the homogeneous background, we consider a dielectric autocorrelation function $B_h(\mathbf{r}-\mathbf{r}')$ arising from a colloidal suspension of small dielectric spheres. This autocorrelation function can be determined using a newly developed technique called *phase space tomography* for optical phase retrieval. This technique measures the optical Wigner distribution function $I(\mathbf{R},\mathbf{k})$ defined as the Fourier transform, with respect to $\mathbf{r}$, of the electric field mutual coherence function $\langle E^*(\mathbf{R}+\mathbf{r}/2)E(\mathbf{R}-\mathbf{r}/2)\rangle_{\text{ensemble}}$. The Wigner distribution function is the wave analog of the specific light intensity, $I^c(\mathbf{R},\hat{k})$, in radiative transfer theory which describes the number of photons in the vicinity of $\mathbf{R}$ propagating in direction $\hat{k}$. The Wigner function describes coherence properties of the electromagnetic field which can propagate much longer than the transport mean-free-path l^* and which are not included in radiative transfer theory. Given the nature of the homogeneous background, repeated light intensity measurements, which determine the optical phase structure at different points along the tissue surface, may be used to determine the size, shape, and internal structure of the inhomogeneity. In principle, this method improves the resolution of optical tomography to the scale of several optical wavelengths in contrast to methods based on diffusion approximation which have a resolution on the scale of several transport mean-free-paths. Our theory, which describes microscopically the wave characteristics of the light, is more fundamental than conventional radiative transfer theory, which treats photons as classical particles. This distinction remains important on scales longer than l^*. Multiple light scattering tomography based on the propagation and measurement of the Wigner distribution function may be useful for the characterization of near-surface tumors.

Keywords multiple light scattering; inhomogeneity; optical tomography.

1 Introduction

Near-infrared optical tomography has recently emerged as a potentially powerful tool in diagnostic medical imaging.[1-9] Unlike well-established x ray imaging and magnetic resonance imaging, which utilize very short wavelength or very long wavelength radiation respectively, the optical method probes an intermediate frequency regime. As emphasized by Chance,[1] this intermediate frequency window facilitates the detection of abnormal metabolic processes leading to tumor formation. This distinguishes the optical method as an early diagnostic tool, from its more established counterparts that respond to structural damage resulting from abnormal metabolism. The description of near-infrared electromagnetic wave propagation in biological tissue is, however, much more complex than for x rays or radio waves. Light exhibits multiple scattering in tissues with a scattering mean-free-path, ℓ, on the scale of 10^{-2} to 10^{-1} mm and a transport mean-free-path, ℓ^*, on the scale of a millimeter. In conventional radiative transfer theory,[9,10] it is convenient to define a specific light intensity, $I^c(\mathbf{R},\hat{k})$, for the number of photons at the point $\mathbf{R}$ travelling in a direction $\hat{k}$. This is analogous to a classical phase space distribution function. It satisfies a phenomenological Boltzmann transport equation. In this model, photons are treated as classical particles that undergo random multiple scattering. It is assumed that the coherent wave nature of the electromagnetic field is lost on the scale of many scattering mean-free-paths ℓ, and from this assumption it follows that on the scale of the transport mean-free-path ℓ^*, photons exhibit classical diffusion.

From a microscopic point of view, the electromagnetic field satisfies a wave equation. In this picture, the classical phase space distribution function (specific intensity) $I^c(\mathbf{R},\hat{k})$ is not well defined.

Address all correspondence to Sajeev John. E-mail: john@physics.utoronto.ca

Wave-particle duality suggests that if the wave vector $\mathbf{k}$ of the photon is specified, its position is uncertain and likewise knowledge of the particle position $\mathbf{R}$ leads to uncertainty in its momentum $\hbar\mathbf{k}$. The nonexistence of a true phase space density motivated Wigner to define the first-order coherence function:[11,12]

$$I(\mathbf{R},\mathbf{k}) \equiv \int d^3\mathbf{r}\, \exp[i\mathbf{k}\cdot\mathbf{r}]\langle E^*(\mathbf{R}+\mathbf{r}/2)$$

$$\times E(\mathbf{R}-\mathbf{r}/2)\rangle_{\text{ensemble}}. \qquad (1)$$

Here, E is the complex electric field amplitude of the propagating radiation field and $\langle\,\rangle_{\text{ensemble}}$ denotes a statistical averaging over all possible realizations of the dielectric microstructure. In this paper we use the terms *specific intensity* and *Wigner coherence function* interchangeably. It must be borne in mind, however, that $I(\mathbf{R},\mathbf{k})$ defined in (1) is not positive definite and that the analogy with conventional Boltzmann transport theory is not exact. It is shown in the appendix that a coarse-grained version of the Wigner function is in fact positive definite and may be identified as a true specific intensity.

It is our aim in this paper to describe the precise integro-differential equation satisfied by the propagator $\Gamma(\mathbf{R}-\mathbf{R}';\mathbf{k},\mathbf{k}')$ of first-order coherence, which is defined as

$$I(\mathbf{R},\mathbf{k}) = \int d^3\mathbf{R}'\, d^3\mathbf{k}'\, \Gamma(\mathbf{R}-\mathbf{R}';\mathbf{k},\mathbf{k}') I_0(\mathbf{R}',\mathbf{k}'),$$

where $I_0(\mathbf{R}',\mathbf{k}')$ is the source coherence function. This $\Gamma(\mathbf{R}-\mathbf{R}';\mathbf{k},\mathbf{k}')$ is equal to an ensemble average of a product of two Green's functions [see Eq. (9) below]. It is the Wigner function detected at $\mathbf{R}$ arising from a source at $\mathbf{R}'$ with specified coherence properties. The transport equation satisfied by Γ turns out to be similar to the classical Boltzmann equation except with nonlocal interactions arising from wave coherence. This result suggests that fundamental distinctions exist between optical tomography based on conventional radiative transfer theory and coherence propagation theory. We find, very remarkably, that for a simple model of multiple-light scattering in a colloidal suspension of polystyrene spheres in water, certain features of the Wigner function propagate coherently on length scales which are on an order of magnitude longer than the transport mean-free-path ℓ^*. This is in contrast to a purely particlelike picture of photons in which purely ballistic propagation is attenuated on the scale of the scattering length $\ell \ll \ell^*$. This suggests that measurement of the Wigner function (optical coherence imaging) may provide a higher degree of sensitivity to properties of the dielectric microstructure than measurement of the total diffuse intensity. Coherence tomography also offers the possibility of higher resolution imaging.

Classical diffusion theory requires coarse graining of the electric field amplitude on sufficiently large length scales that the true wave characteristics of transport are no longer apparent. The Wigner function, however, allows resolution on the scale of the optical wavelength. These features of coherence tomography are of value to both time- and frequency-domain studies[5,7] of biological tissue. In the case of multiple light scattering from an inhomogeneity (tumor) in an otherwise homogeneously disordered medium, the Wigner function behaves like a quantum mechanical wave function which scatters from the effective potential presented by the inhomogeneity. This facilitates a description of transport which in many respects resembles that of scattering of a quantum particle in a uniform background by a fixed impurity.

The possibility of measuring the Wigner coherence function using purely intensity measurements and refractive optics (lenses) has been demonstrated by Raymer, Beck, and McAlister.[13] The method uses a series of measurements of the light intensity at a point on the sample surface imaged by a pair of lenses to reconstruct uniquely, by tomographic reconstruction, the full Wigner coherence function at that point. Passage of the light through a pair of lenses effects a Fresnel integral transformation of the wave amplitude on the sample surface. This is equivalent to a projection integral of the Wigner coherence function. By varying the position of the lenses, a variety of different tomographic projections may be obtained, leading to reconstruction of the Wigner function by inverse Radon transform. This method can be repeated at a variety of different points along the sample surface, thereby yielding a detailed map of optical absorption and dielectric microstructure within the sample.

Light scattering from an inhomogeneity in an otherwise nonscattering background medium readily yields valuable information about the location and nature of the inhomogeneity. In the case of a weak inhomogeneity, the single scattering differential cross-section is related to Fourier components of the dielectric inhomogeneity evaluated at the photon wave-vector transfer $\mathbf{q}=\mathbf{k}_f-\mathbf{k}_i$. For a dielectric fluctuation described by the function $\epsilon_{\text{fluct}}(\mathbf{r})$, the light intensity scattered from the incident wave vector $\mathbf{k}_i$ to the final wave vector $\mathbf{k}_f$ is given by (in Dirac notation) $|\langle\mathbf{k}_f|\epsilon_{\text{fluct}}(\mathbf{r})|\mathbf{k}_i\rangle|^2$ in the first Born approximation.

A similar situation is encountered in the scattering of an electron from a central potential $V(|\mathbf{r}|)$.[14] The scattering of the coherent de Broglie wave of the electron can be characterized by a series of phase shifts, δ_ℓ, for each of the angular momentum partial waves of an incident plane wave. As a function of the electron energy, the set of phase shifts provides a fingerprint of the scattering potential $V(|\mathbf{r}|)$. This is based on the decomposition of the

incident coherent wave of wave vector $\mathbf{k}_i \equiv k\hat{z}$ into angular momentum components:

$$\exp[ikz] = \sum_{\ell=0}^{\infty} (2\ell+1)i^\ell j_\ell(kr) P_\ell(\hat{k}_i \cdot \hat{r}). \quad (2)$$

This is independent of the strength of the potential, and the scattering is usually dominated by a finite number $\ell \leq \ell_{max}$ of partial waves.

The simplicity of the scattering problem when the background medium is uniform (and nonscattering) arises from the fact that Green's function for the amplitude of a coherent wave of frequency $\omega = ck$ is given by[14]

$$G_0^{\pm}(\mathbf{r},\mathbf{r}') = -\frac{1}{4\pi} \frac{\exp[\pm ik|\mathbf{r}-\mathbf{r}'|]}{|\mathbf{r}-\mathbf{r}'|} \quad (3)$$

and that this is in turn has a straightforward partial wave expansion. If the background is itself a scattering medium, the propagation of energy in the wave field may be described in a statistical sense. This follows from multiple scattering theory and ensemble averaging over the possible configurations of the dielectric disorder $\epsilon_h(\mathbf{r})$ with an appropriate statistical weight. The statistical properties of the background are given by the translationally invariant, ensemble-averaged autocorrelation function:

$$B_h(\mathbf{r}-\mathbf{r}') \equiv \frac{\omega^4}{c^4} \langle \epsilon_h^*(\mathbf{r})\epsilon_h(\mathbf{r}') \rangle_{ensemble}. \quad (4)$$

Green's function of wave intensity $I(\mathbf{R}) \equiv \langle |E(\mathbf{R})|^2 \rangle_{ensemble}$ can then be derived using the methods of multiple scattering theory. Here $E(\mathbf{R})$ is the electric field amplitude of the electromagnetic wave point $\mathbf{R}$. For a source at point $\mathbf{R}'$ and a source to detector separation $L \equiv |\mathbf{R}-\mathbf{R}'| \gg \ell^*$, where ℓ^* is the transport mean-free-path, the total light intensity detected at $\mathbf{R}$ is given by Green's function of the diffusion equation:

$$I(\mathbf{R}) = \frac{1}{4\pi D_0 |\mathbf{R}-\mathbf{R}'|}. \quad (5)$$

Here D_0 is the optical diffusion coefficient. In this description, the coherent wave properties of the underlying electromagnetic field have been integrated over. The intensity (5) described by the diffusion model is the wave-vector integral of the Wigner coherence function[11] $I(\mathbf{R},\mathbf{k})$:

$$I(\mathbf{R}) \equiv \int \frac{d^3\mathbf{k}}{(2\pi)^3} I(\mathbf{R},\mathbf{k}). \quad (6)$$

Here $\mathbf{k}$ is a wave vector describing local wave propagation in the direction $\hat{k}$ and $\mathbf{R}$ describes a coarse-grained region with linear dimensions greater than the optical wavelength, λ, but smaller than a few transport mean-free-paths, ℓ^*. As shown in the appendix, a generalized coarse-

graining procedure applied to $I(\mathbf{R},\mathbf{k})$, which implements the fundamental uncertainty relation $\Delta R \Delta k \geq 1$, leads to the conventional specific intensity $I^c(\mathbf{R},\mathbf{k})$.

It is our aim to generalize the diffusion Green's function (5) for the total light intensity, $I(\mathbf{R})$, to the Wigner distribution function, $I(\mathbf{R},\mathbf{k})$ and to elucidate the relationship of Green's function for the Wigner coherence to the autocorrelation function $B_h(\mathbf{r}-\mathbf{r}')$. To the extent that $I(\mathbf{R},\mathbf{k})$ can be measured experimentally, the nature of the homogeneous scattering medium can be determined with a resolution scale given by the wavelength of light λ. This can be several orders of magnitude better than the resolution scale ($\gtrsim \ell^*$) afforded by the diffusion model.

A tumor in biological tissue can be described as a localized statistical inhomogeneity:

$$B(\mathbf{r}_1,\mathbf{r}_2) \equiv \frac{\omega^4}{c^4} \langle \epsilon^*(\mathbf{r}_1)\epsilon(\mathbf{r}_2) \rangle_{ensemble}$$

$$= B_h(\mathbf{r}) + V(\mathbf{R})B_i(\mathbf{r}), \quad (7)$$

where

$$\mathbf{r} = \mathbf{r}_1 - \mathbf{r}_2, \quad \mathbf{R} = (\mathbf{r}_1 + \mathbf{r}_2)/2.$$

Here $V(\mathbf{R})$ is a function that vanishes outside of the region of the tumor and describes its shape and strength. $B_i(\mathbf{r})$ describes the change in scattering and absorption within the tumor region from their values in the background. In this paper, we demonstrate that multiple light scattering from a statistical inhomogeneity of the form (7) can be reduced to a quantum scattering problem and can be described in terms of a series of partial waves and scattering amplitudes. Given the nature of the homogeneously disordered background $B_h(\mathbf{r})$, it is possible to relate the scattering amplitudes to the overall tumor profile $V(\mathbf{R})$ as well as its internal characteristic function $B_i(\mathbf{r})$. This leads to a much more detailed characterization cell structure within the tumor than is possible using either a diffusion model or radiative transfer theory. The functions $B_i(\mathbf{r})$ and $B_h(\mathbf{r})$ describe in detail absorption and cell structure, inside and outside the tumor region.

2 WAVE PROPAGATION IN A HOMOGENEOUSLY DISORDERED BACKGROUND TISSUE

We first review the multiple scattering theory of light in an isotropic, homogeneously disordered dielectric material.[15,16] This is a microscopic wave propagation theory which is more fundamental than radiative transfer theory or Boltzmann transport theory.[10] It directly relates Green's function for Wigner coherence, $\Gamma_h(\mathbf{R}-\mathbf{R}',\mathbf{k},\mathbf{k}')$, to the microscopic correlation function $B_h(\mathbf{r})$. Here Γ_h is the correlation function of Wigner coherence for light emitted with wave vector $\mathbf{k}'$ from a source at $\mathbf{R}'$

and the light detected at point $\mathbf{R}$, with wave vector $\mathbf{k}$. This provides much greater information than the diffusion theory that relates the total light intensity correlations to the transport mean-free-path ℓ^*. Accordingly, multiple scattering theory requires the measurement of the two-point electric field autocorrelation function $\langle E^*(\mathbf{r}_1)E(\mathbf{r}_2)\rangle_{\text{ensemble}}$ rather than the one-point intensity $\langle |E(\mathbf{r})|^2\rangle_{\text{ensemble}}$ where the two-point separation $|\mathbf{r}_1 - \mathbf{r}_2|$ is small compared to a few transport mean-free-paths. This autocorrelation function $\langle E^*(\mathbf{r}_1)E(\mathbf{r}_2)\rangle_{\text{ensemble}}$ can be measured experimentally by phase space tomography and the technique of fractional-order Fourier transforms.[11–13]

We consider a model dielectric medium consisting of a random liquidlike arrangement of identical dielectric spheres in water.[17] The Fourier transform of $B_h(\mathbf{r})$ is given by

$$\tilde{B}_h(\mathbf{q}) = \frac{\omega^4}{c^4} |b(\mathbf{q})|^2 S(\mathbf{q}). \qquad (8)$$

Here $|b(\mathbf{q})|^2$ is the form factor (sometimes referred to as the phase function) describing scattering from the individual dielectric spheres and $S(\mathbf{q})$ is the structure factor describing the statistical arrangement of the collection of spheres in the medium. We employ a Percus-Yevick approximation[17] to describe $S(\mathbf{q})$. The position and height of various peaks in $S(\mathbf{q})$ as a function of $q \equiv |\mathbf{q}|$ are sensitively determined by the volume-filling fraction, ϕ, of spheres. For a dilute ($\phi \lesssim 0.25$) collection of spheres with refractive index $n \simeq 1.5$, and diameter comparable to the optical wavelength, the function $\tilde{B}_h(\mathbf{q})$ contains detailed microscopic information about the dielectric medium on scales small compared to ℓ^*. The diffusion model is insensitive to this information. We describe how multiple scattering spectroscopy may resolve the medium characteristics at the scale of the optical wavelength.

Consider an extended source in the vicinity of point $\mathbf{R}'$ containing the points $\mathbf{r}_1'$ and $\mathbf{r}_2'$. The electric field generated by the extended source at point $\mathbf{r}'$ is denoted by $E_0(\mathbf{r}')$ and $\mathbf{R}' \equiv (\mathbf{r}_1' + \mathbf{r}_2')/2$. The resulting electric field amplitude is measured by an extended detector in the vicinity of point $\mathbf{R} = (\mathbf{r}_1 + \mathbf{r}_2)/2$. The resulting electric field autocorrelation function is given by

$$\langle E(\mathbf{r}_1)E^*(\mathbf{r}_2)\rangle_{\text{ensemble}}$$

$$= \frac{\omega^4}{c^4} \int_{\mathbf{r}_1'\mathbf{r}_2'} \langle G^+(\mathbf{r}_1,\mathbf{r}_1')G^-(\mathbf{r}_2,\mathbf{r}_2')\rangle_{\text{ensemble}}$$

$$\times E_0(\mathbf{r}_1')E_0^*(\mathbf{r}_2'). \qquad (9)$$

Here, and throughout this article, we use the notation $\int d^3\mathbf{r} \equiv \int_{\mathbf{r}}$ for coordinate space integrals and the notation $\int [d^3\mathbf{k}/(2\pi)^3] \equiv \int_{\mathbf{k}}$ for wave-vector integrals. For a source-emitting light with initial wave vector $\mathbf{k}'$, the product of electric fields in the source region may be rewritten as

$$E_0(\mathbf{r}_1')E_0^*(\mathbf{r}_2') = I_0(\mathbf{R}',\mathbf{k}')\exp[i\mathbf{k}'\cdot(\mathbf{r}_1' - \mathbf{r}_2')], \qquad (10)$$

where I_0 is the Wigner coherence function of the source. Green's functions in Eq. (9) are solutions of the wave equation:

$$\left[-\nabla^2 - \frac{\omega_{\pm}^2}{c^2}\epsilon_h(\mathbf{r}) \right] G^{\pm}(\mathbf{r},\mathbf{r}_1) = \delta(\mathbf{r} - \mathbf{r}_1'), \qquad (11)$$

where $\omega_{\pm} \equiv \omega + i\eta$ with $\eta \rightarrow 0$. It follows from Eqs. (9) and (10) that

$$I(\mathbf{R},\mathbf{k}) = \int_{\mathbf{R}',\mathbf{k}'} \Gamma_h(\mathbf{R} - \mathbf{R}';\mathbf{k},\mathbf{k}')I_0(\mathbf{R}',\mathbf{k}'). \qquad (12)$$

The microscopic form of the kernel Γ_h follows from carrying out perturbation theory in the effective "scattering potential" $(\omega^2/c^2)\epsilon_h(\mathbf{r})$ and taking the ensemble average defined by Eq. (4). The details of this derivation may be found elsewhere.[15,16] The derivation of the transport equation involves the summation of an infinite series of terms. These terms describe different multiple scattering paths taken by the photons. In the case of weak scattering, defined by the criterion $\lambda \ll \ell^*$, it is reasonable to neglect the interference between different scattering paths on length scales $L \gg \ell^*$. Consider for instance, the electric field amplitude arriving at the detector from two independent paths labelled 1 and 2, with amplitudes A_1 and A_2 respectively. These amplitudes can be expressed as

$$A_n = f_n \exp\left[i\sum_j \mathbf{q}_j^{(n)}\cdot\mathbf{r}_j^{(n)}(t)\right], \quad n = 1,2,$$

where $\{\mathbf{r}_j^{(n)}(t)\}$ are the positions of the scattering events on path n, which can be a function of the time variable t due to random thermal motion of the scatterers. In biological tissue, in addition to thermal fluctuations, nonequilibrium processes such as the flow of fluids and blood cells lead to time variations in $\mathbf{r}_j^{(n)}$. Here, $\mathbf{q}_j^{(n)}$s are the related scattering wave vectors, and f_ns are constant factors that account for the scattering strength of each scattering event. The intensity detected is given by time averaging of $|A_1 + A_2|^2$ over the time scale of measurement, which we denote as τ. In particular,

$$\langle |A_1 + A_2|^2\rangle_{\text{time}} = \langle |A_1|^2 + |A_2|^2\rangle_{\text{time}}$$

$$+ \langle A_1 A_2^* + A_1^* A_2\rangle_{\text{time}}. \qquad (13)$$

The interference term $A_1 A_2^* + A_1^* A_2$ can be either positive or negative with equal likelihood. For the model of Brownian motion, the result of averaging is given by[16]

$$\langle A_1 A_2^* + A_1^* A_2\rangle_{\text{time}} = A_{12}(0)\exp[-N\langle q^2\rangle D_s \tau].$$

Here $A_{12}(0)$ is the value of the interference term at $t = 0$, $\langle q^2\rangle$ is the average value of $\mathbf{q}_j^{(n)}\cdot\mathbf{q}_j^{(n)}$ with respect to the scatterer form factor $|b(\mathbf{q})|^2$, D_s is the diffusion coefficient for the scatterers, and N is the

total number of scattering events on both paths. The time scale $t_0 \equiv (\langle q^2 \rangle D_s)^{-1}$ is the time for the scattering particles to diffuse a distance on the order of an optical wavelength. It is clear that for $N\tau \gg t_0$ this interference term vanishes (with the exception of paths contributing to coherent backscattering).[18,19] For a diffusive scattering path, $N \simeq (L/\ell)^2$, where L is the thickness of the illuminated sample and ℓ is the scattering mean-free-path. The criterion, $\tau \gg t_0(\ell/L)^2$, for neglecting interference effects may be violated in certain exceptional cases such as in the case of ultrashort optical pulse duration τ or in the case of relatively static tissue such as the human tooth.

The neglect of interference effects between different scattering paths leads to an elementary partial wave expansion for the transport kernel Γ_h. This is analogous to the partial wave expansion (2) of the plane wave amplitude in a nonscattering medium. In the present case, it is an expansion of the coherence function $\langle E(\mathbf{r}_1)E^*(\mathbf{r}_2)\rangle_{\mathrm{ensemble}}$ rather than direct amplitude $E(\mathbf{r})$. The result[20] of this expansion is

$$\Gamma_h(\mathbf{R}-\mathbf{R}';\mathbf{k},\mathbf{k}')$$

$$\simeq \sum_{m=-\ell_{\max}}^{\ell_{\max}} \sum_{\ell,\ell'=|m|}^{\ell_{\max}} \frac{\exp[-|\mathbf{R}-\mathbf{R}'|/\lambda_{\ell\ell'}^{[m]}]}{4\pi D_{\ell\ell'}^{[m]}|\mathbf{R}-\mathbf{R}'|^{(1+|\ell-\ell'|)}}$$

$$\times \psi_{\ell m}^*(\mathbf{k})\psi_{\ell'm}(\mathbf{k}'). \qquad (14)$$

The $\ell=\ell'=m=0$ term corresponds to the isotropic diffusion mode. $D_{00}^{[0]}$ is the optical diffusion coefficient, $\lambda_{00}^{[m]}=\infty$ and $\psi_{00}(\mathbf{k})$ is a function that is highly peaked in the vicinity of $k_0=|\mathbf{k}|=\omega/c$ and independent of the direction $\hat{k}$.

The terms with $\ell=\ell'\geqslant1$ correspond to higher angular momentum partial waves of the coherence Green's function and, in general, the spectral functions take the form

$$\psi_{\ell m}(\mathbf{k})=R_\ell(k)Y_\ell^m(\hat{k}), \qquad (15)$$

where $Y_\ell^m(\hat{k})$ is a spherical harmonic and $R_\ell(k)$ is a "radial" function that is highly peaked in the vicinity of k_0. For $\ell=\ell'\geqslant1$, the length scale parameters $\lambda_{\ell\ell'}^{[m]}$ are finite. For instance, $\lambda_{11}^{[0]}$ is on the order of several transport mean-free-paths and, in general, $\lambda_{\ell\ell'}^{[m]}$ decreases when ℓ is increased. The $\ell\neq\ell'$ terms in (14) correspond to the transitions among different modes, and the parameters $\lambda_{\ell\ell'}^{[m]}$ are finite, in general, except for those with ℓ or $\ell'=0$. (When one of the ℓ and ℓ' is equal to zero, $\lambda_{\ell\ell'}^{[0]}=\infty$). The parameters $\lambda_{\ell\ell'}^{[m]}$ for $\ell,\ell'\geqslant1$ describe the length scale on which nondiffusive coherence effects propagate through the medium on average. On very long length scales $|\mathbf{R}-\mathbf{R}'|\gg\lambda_{11}^{[0]}$, only the diffusion mode persists, whereas on shorter length scales coherence properties are observable. Equation (14) therefore provides a microscopic interpolation scheme from the "diffusive," to "snakelike,"

to "ballistic" photons (in the purely particle picture) as the source to detector separation is decreased, or equivalently the time gating[6] of detected photons is changed. The length scales $\lambda_{\ell\ell'}^{[m]}$, the weight factor $D_{\ell\ell'}^{[m]}$, and the spectral functions $\psi_{\ell m}(\mathbf{k})$ can be microscopically related to the characteristic function of the medium $B_h(\mathbf{r})$.

Equation (14) is derived by using the multiple scattering theory.[15,16] We first define

$$\tilde{\Gamma}_h(\mathbf{Q};\mathbf{k}',\mathbf{k})\equiv k_0^{-4}\int d^3\mathbf{R}\,\exp[-i\mathbf{Q}\cdot\mathbf{R}]\Gamma_h(\mathbf{R},\mathbf{k}',\mathbf{k}),$$

$$k_0\equiv\omega/c. \qquad (16)$$

Here, the input and output photon wave vectors $\mathbf{k}'$ and $\mathbf{k}$ may be thought of as continuous indices of the matrix $\tilde{\Gamma}_h$, and $\mathbf{Q}$ as the "inverse" source-detector vector in reciprocal space. The matrix Γ_h describes the transfer of radiation at wave vector $\mathbf{k}'$ to wave vector $\mathbf{k}$ through a sequence of intermediate wave vectors. Multiple scattering theory[15,16] (neglecting the interference of different radiative transfer paths) leads to the result that $\tilde{\Gamma}_h$ is given by the inverse of the operator (matrix):

$$H\equiv f_\mathbf{Q}(\mathbf{k})-B_h(\mathbf{r}), \qquad (17)$$

where

$$f_\mathbf{Q}(\mathbf{k})=\left[k_0^2-\left(\mathbf{k}+\frac{\mathbf{Q}}{2}\right)^2-\Sigma^+\left(\mathbf{k}+\frac{\mathbf{Q}}{2}\right)\right]$$

$$\times\left[k_0^2-\left(\mathbf{k}-\frac{\mathbf{Q}}{2}\right)^2-\Sigma^-\left(\mathbf{k}-\frac{\mathbf{Q}}{2}\right)\right]$$

and

$$\Sigma^\pm(\mathbf{k})=\int_\mathbf{q}\tilde{B}_h(\mathbf{k}-\mathbf{q})/[k_0^2-q^2-\Sigma^\pm(\mathbf{q})].$$

In particular,

$$\tilde{\Gamma}_h(\mathbf{Q};\mathbf{k}',\mathbf{k})=\langle\mathbf{k}'|H^{-1}|\mathbf{k}\rangle. \qquad (18)$$

The operator H is analogous to the Hamiltonian of a quantum mechanical particle moving in the potential well $-B_h(\mathbf{r})$ with an energy versus wave vector (dispersion) relation given by $f_\mathbf{Q}(\mathbf{k})$. The transport kernel (14) follows from solving (18) by using the eigenfunctions of H at $Q=0$ as basis functions. The "ground state" energy of H at $Q=0$ is rigorously equal to zero (in the absence of absorption). This corresponds to the isotropic and undamped diffusion mode.

We find that the eigenvalue spectrum of H at $Q=0$ is especially simple in the case of (weak) scattering pertinent to biological tissue. In general, the eigenvalue spectrum of a three-dimensional potential well consists of bound states and continuum states. The bound states are labelled by a principal quantum number n and angular momentum quan-
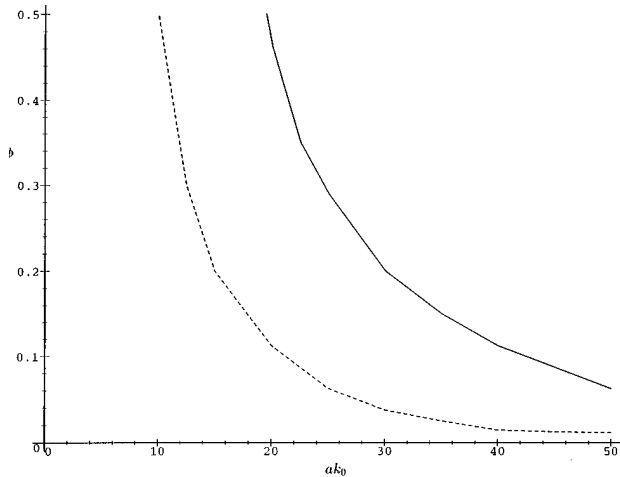
Fig. 1 Parameter region (the one under each curve) in which the bound state spectrum contains only the $n=0$ principal quantum number. The calculation was carried out for the model of identical dielectric spheres in water, with relative refractive indexes 1.09 (the solid line) and 1.193 (the dashed line). ϕ is the volume-filling fraction and a is the radius of the spheres.

tum numbers ℓ and m. In general there are many possible values of n in the bound state spectrum. For the model of identical dielectric spheres in water, with statistical correlations described by the Percus-Yevick approximation, we find that the bound state spectrum contains only the $n=0$ principle quantum number in a certain parameter region, as shown in Figure 1 (the region under each curve) for spheres with a relative refractive index 1.09 (the solid line) and 1.193 (the dashed line). In this figure, a is the radius of the spheres and ϕ is the volume-filling fraction of spheres. For a 10% volume fraction of polystyrene spheres in water (with a relative refractive index 1.193), it requires that $a \lesssim 4\lambda$ (where $\lambda = 2\pi/k_0$ is the optical wavelength) in order to have only the $n=0$ bound states. This essentially requires that the scattering be weak and that the scattering microstructures be no more than an order of magnitude larger than the wavelength of light. In constructing the transport kernel (14) we have included only the $n=0$ bound states. The contribution from continuum states of H to the kernel (14) is negligible, since these modes are exponentially damped on the scale of the wavelength.

The parameters $\lambda_{\ell\ell'}^{[m]}$ and $D_{\ell\ell'}^{[m]}$ in the kernel (14) are determined by the correlation function $B_h(\mathbf{r})$ and they can be calculated numerically once the function $B_h(\mathbf{r})$ is given. Table 1 gives an example for this calculation. In this example, we consider the model of identical polystyrene spheres* in water, with statistical correlations described by the Percus-Yevick approximation. We choose the radius of the

spheres $a = 20k_0^{-1}$ and the volume-filling fraction $\phi = 0.1$ in the calculation. The ℓ and ℓ^* in Table 1 are the related scattering mean-free-path and transport mean-free-path, respectively. We see that $\lambda_{11}^{[0]}$ is the largest among all $\lambda_{\ell\ell'}^{[m]}$, and it is about twenty times larger than the transport mean-free-path! This means that the $\ell = \ell' = 1$ and $m = 0$ term in (14) can propagate for a distance much longer than the transport mean-free-path in this example. For this particular choice of a and ϕ, we find that $D_{00}^{[0]}/D_{11}^{[0]} \simeq .054$. In other words, the $\ell = 1$ mode amplitude is only 1.5 orders of magnitude smaller than the $\ell = 0$ mode. From Table 1, we also see that $\lambda_{22}^{[m]}$ and $\lambda_{33}^{[m]}$ are much smaller than $\lambda_{11}^{[0]}$, while some off-diagonal elements, such as $\lambda_{13}^{[0]}$, are close to $\lambda_{11}^{[0]}$ in value. If we change the function $B_h(\mathbf{r})$ by changing, for instance, the radius or the refractive index of the spheres, the $\lambda_{11}^{[0]}$ and the other coherence lengths will change their values accordingly. Table 2 shows how the quantities $\lambda_{11}^{[0]}/\ell^*$ and $\lambda_{33}^{[0]}/\ell^*$ change when we change the parameters a, ϕ and $\Delta\epsilon$ (where $\Delta\epsilon$ is the ratio of the dielectric constant of the spheres to that of water). We see from Table 2 that, for fixed ϕ and $\Delta\epsilon$, $\lambda_{11}^{[0]}/\ell^*$ first increases and then decreases when we increase parameter a, and $a = 20k_0^{-1}$ (with $\phi = 0.1$ and $\Delta\epsilon = 1.423$) corresponds to the maximum value of $\lambda_{11}^{[0]}/\ell^*$ in this table. We also see that, in Table 2, $\lambda_{11}^{[0]}/\ell^*$ increases when we increase ϕ or $\Delta\epsilon$. Owing to the dependence of $\lambda_{\ell\ell'}^{[m]}$ on the function $B_h(\mathbf{r})$, it is possible to use the observable parameters $\lambda_{\ell\ell'}^{[m]}$, as well as $D_{\ell\ell'}^{[m]}$, to characterize the medium properties contained in $B_h(\mathbf{r})$.

We mention that the neglect of interference between different radiative transfer paths in (13) is a good approximation with the exception of the back-scattering direction. Here it is well known that the coherent interference of "time-reversed" optical paths can give rise to an intensity peak in retroreflection from a disordered, dielectric half-space.[18,19] This peak intensity is up to twice the "diffuse" background and has an angular width that is of the order (λ/ℓ^*) radians. Accordingly, the interference corrections to the transport theory we have outlined are of the order $(\lambda/\ell^*)^2$. For biological tissue, with a transport mean-free-path $\ell^* \sim 1$ mm and at wavelengths $\lambda \sim 1$ μm, this correction is very small. Nevertheless, a generalization of (17) to include the effects of coherent backscattering is possible. This, however, leads to the complication that the local "potential" $B_h(\mathbf{r})$ must be replaced by a nonlocal "potential."[20]

In the above paragraphs we described wave propagation in an isotropically disordered homogeneous background without absorption. In the presence of absorption, the dielectric constant $\epsilon_h(\mathbf{r})$ is no longer real and has an imaginary part. It can be shown[20] that the corresponding Green's function for Wigner coherence in this case is of the same form as (14) but the coherence lengths $\lambda_{\ell\ell'}^{[m]}$, espe-

---

*The ratio of the dielectric constant of polystyrene spheres to that of water is 1.423.

Table 1 Numerical results of the coherent lengths $\lambda_{\ell\ell'}^{[m]}$, the scattering mean-free-path ℓ, and the transport mean-free-path ℓ^* for the model of identical polystyrene spheres in water, with statistical correlations described by the Percus-Yevick approximation.

ℓ	ℓ^*	m	$\lambda_{11}^{[m]}$	$\lambda_{22}^{[m]}$	$\lambda_{33}^{[m]}$	$\lambda_{12}^{[m]}$	$\lambda_{13}^{[m]}$	$\lambda_{23}^{[m]}$
7.4	6.0×10^2	0	$\simeq1.1\times10^4$	2.0×10^2	2.0×10^2	$\simeq7.6\times10^3$	$\simeq8.5\times10^3$	2.0×10^2
		1	3.6×10^2	4.7×10^2	1.9×10^2	4.6×10^2	$\simeq1.2\times10^3$	4.6×10^2

Note: The radius of the spheres and the volume-filling fraction are taken to be $20k_0^{-1}$ and 0.1, respectively. We set $\ell_{max}=3$ in the calculation. All lengths are in units of k_0^{-1}.

cially, $\lambda_{00}^{[0]}$, $\lambda_{0\ell}^{[0]}$ and $\lambda_{\ell0}^{[0]}$, now are all finite. This is because the ground state energy of H_0 is no longer equal to zero in dissipative media.

We note, finally, that in this paper we have considered only the case of time-independent, steady-state imaging. For frequency-domain or time-domain imaging, we need to consider the time-dependent generalization of Eqs. (16) to (18). For example, to describe modulation of the source intensity at the frequency Ω, it is necessary to evaluate the advanced and retarded self-energies $\Sigma^\pm$ at frequencies $ck_0+\Omega/2$ and $ck_0-\Omega/2$ respectively, rather than at the same frequency ck_0. A detailed discussion of frequency-domain and time-domain measurements is given in Ref. 20.

3 COMPARISON WITH CONVENTIONAL RADIATIVE TRANSFER THEORY

In this section we compare our wave theory described in the previous section with conventional radiative transfer theory. As mentioned earlier, our theory is more fundamental than conventional radiative transfer theory.[10] Here, we elucidate the important differences. For this purpose, we first rewrite (18) as the following integral equation[20]

$$2\mathbf{k}\cdot\mathbf{Q}\tilde{\Gamma}_h(\mathbf{Q};\mathbf{k},\mathbf{k}')$$

$$=\Delta G_{\mathbf{k}}(\mathbf{Q})\delta_{\mathbf{k}\mathbf{k}'}+\int_{\mathbf{k}_1}\Delta G_{\mathbf{k}}(\mathbf{Q})\tilde{B}_h(\mathbf{k}-\mathbf{k}_1)\tilde{\Gamma}_h(\mathbf{Q};\mathbf{k}_1,\mathbf{k}')$$

$$-\left(\int_{\mathbf{k}_1}\Delta G_{\mathbf{k}_1}(\mathbf{Q})\tilde{B}_h(\mathbf{k}-\mathbf{k}_1)\right)\tilde{\Gamma}_h(\mathbf{Q};\mathbf{k},\mathbf{k}'), \qquad (19)$$

where

$$\Delta G_{\mathbf{k}}(\mathbf{Q})\equiv G^+(\mathbf{k}+\mathbf{Q}/2)-G^-(\mathbf{k}-\mathbf{Q}/2),$$
$$(20)$$
$$G^\pm(\mathbf{k})\equiv[k_0^2-k^2-\Sigma^\pm(\mathbf{k})]^{-1}.$$

Equation (19) is equivalent to (18) and can be derived by using (17) and (20).

On the other hand, in conventional radiative transfer theory, the (time-independent) specific light intensity $I^c(\mathbf{R},\mathbf{k})$ (where the index c denotes conventional radiative transfer theory) of a homogeneous medium without absorption satisfies the following phenomenological Boltzmann transport equation[9,10]

Table 2 Ratios of coherence lengths $\lambda_{11}^{[0]}$ and $\lambda_{33}^{[0]}$ to transport mean-free-path ℓ^* versus parameters ϕ—the volume-filling fraction, a—the radius of the spheres, and $\Delta\epsilon$—the ratio of dielectric constant of the spheres to that of water.

Parameters						
$\Delta\epsilon$	ϕ	ak_0	ℓk_0	$\ell^* k_0$	$\lambda_{11}^{[0]}/\ell^*$	$\lambda_{33}^{[0]}/\ell^*$
1.423	0.1	10	2.0×10^1	4.9×10^2	12.8	0.21
1.423	0.1	20	7.4	6.0×10^2	18.0	0.33
1.423	0.1	27	8.9	1.2×10^3	11.4	0.26
1.193	0.1	20	4.5×10^1	3.7×10^3	3.0	0.21
1.1	0.1	20	1.8×10^2	1.5×10^4	0.7	0.15
1.193	0.3	20	2.7×10^1	1.4×10^3	5.0	0.24
1.193	0.05	20	7.9×10^1	7.2×10^3	1.5	0.20

$$(\mathbf{k}\cdot\nabla_{\mathbf{R}})I^c(\mathbf{R},\mathbf{k})+k\sigma(k)I^c(\mathbf{R},\mathbf{k})$$

$$=I_0^c(\mathbf{R},\mathbf{k})+\int_{\mathbf{k}'}k'\sigma(\mathbf{k}'\rightarrow\mathbf{k})I^c(\mathbf{R},\mathbf{k}'), \qquad (21)$$

where $\sigma(k)$ and $\sigma(\mathbf{k}'\rightarrow\mathbf{k})$ are the total and angular scattering coefficients, respectively, and satisfy the relation

$$\int_{\mathbf{k}'}\sigma(\mathbf{k}\rightarrow\mathbf{k}')=\sigma(k). \qquad (22)$$

In (21), $I_0^c(\mathbf{R},\mathbf{k})$ is the source-specific intensity. Now, if we define

$$I^c(\mathbf{R},\mathbf{k})=\int_{\mathbf{R}'\mathbf{k}'}\Gamma_h^c(\mathbf{R}-\mathbf{R}';\mathbf{k},\mathbf{k}')I_0^c(\mathbf{R}',\mathbf{k}'), \quad (23)$$

then we can show from (21) that the Fourier transform of $\Gamma_h^c(\mathbf{R}-\mathbf{R}';\mathbf{k},\mathbf{k}')$ satisfies

$$i\mathbf{k}\cdot\mathbf{Q}\Gamma_h^c(\mathbf{Q};\mathbf{k},\mathbf{k}')=\delta_{\mathbf{k}\mathbf{k}'}+\int_{\mathbf{k}_1}k_1\sigma(\mathbf{k}_1\rightarrow\mathbf{k})$$

$$\times\tilde{\Gamma}_h^c(\mathbf{Q};\mathbf{k}_1,\mathbf{k}')-k\sigma(k)$$

$$\times\tilde{\Gamma}_h^c(\mathbf{Q};\mathbf{k},\mathbf{k}'). \qquad (24)$$

It can be easily seen that (19) and (24) are equivalent if we ignore the Q dependence of $\Delta G_{\mathbf{k}}(\mathbf{Q})$ in (19) and identify

$$\tilde{\Gamma}_h(\mathbf{Q};\mathbf{k},\mathbf{k}')\leftrightarrow\tilde{\Gamma}_h^c(\mathbf{Q};\mathbf{k},\mathbf{k}')[i\Delta G_{\mathbf{k}'}(0)]/2,$$

$$\sigma(k)\leftrightarrow\frac{1}{2k}\int_{\mathbf{k}_1}\tilde{B}_h(\mathbf{k}-\mathbf{k}_1)[i\Delta G_{\mathbf{k}_1}(0)]=-\mathrm{Im}\Sigma^+(k)/k,$$

$$\sigma(\mathbf{k}'\rightarrow\mathbf{k})\leftrightarrow\frac{1}{2k'}[i\Delta G_{\mathbf{k}}(0)]\tilde{B}_h(\mathbf{k}-\mathbf{k}'). \qquad (25)$$

Therefore, the conventional radiative transfer theory ignores[†] the $\mathbf{Q}$ dependence of $\Delta G_{\mathbf{k}}(\mathbf{Q})$, which corresponds to a nonlocal interaction in position space, as shown in Fig. 2 where we plot the Fourier transform of $i\Delta G_{\mathbf{k}}(\mathbf{Q})$ for some fixed $\mathbf{k}$'s in the forward direction [in the backward direction, with $\mathbf{k}\cdot\mathbf{R}<0$, the Fourier transform of $i\Delta G_{\mathbf{k}}(\mathbf{Q})$ oscillates rapidly on the scale of the wavelength]. Owing to the neglect of $\mathbf{Q}$ dependence, the propagator $\Gamma_h(\mathbf{R}-\mathbf{R}';\mathbf{k},\mathbf{k}')$ given by conventional radiative transfer theory differs from that obtained from our wave theory in the following two respects[20]: (1) The related terms with $m=0, \ell=1$ and $\ell'\geq 1$ as well as the terms with $m=0,\ell'=1$ and $\ell\geq 1$ in (14) are completely missing in the conventional radiative transfer theory. In particular, the term with $m=0$ and $\ell=\ell'=1$, which can usually propagate for a much

---

[†]One consequence of ignoring the $\mathbf{Q}$ dependence of $\Delta G_{\mathbf{k}}(\mathbf{Q})$ in the conventional radiative transfer theory is that the diffusion coefficient D_0, in the limit of length scales much larger than l^*, comes only from the coupling between ψ_{00} and ψ_{01}, the ground state and the first excited state of H at $Q=0$.
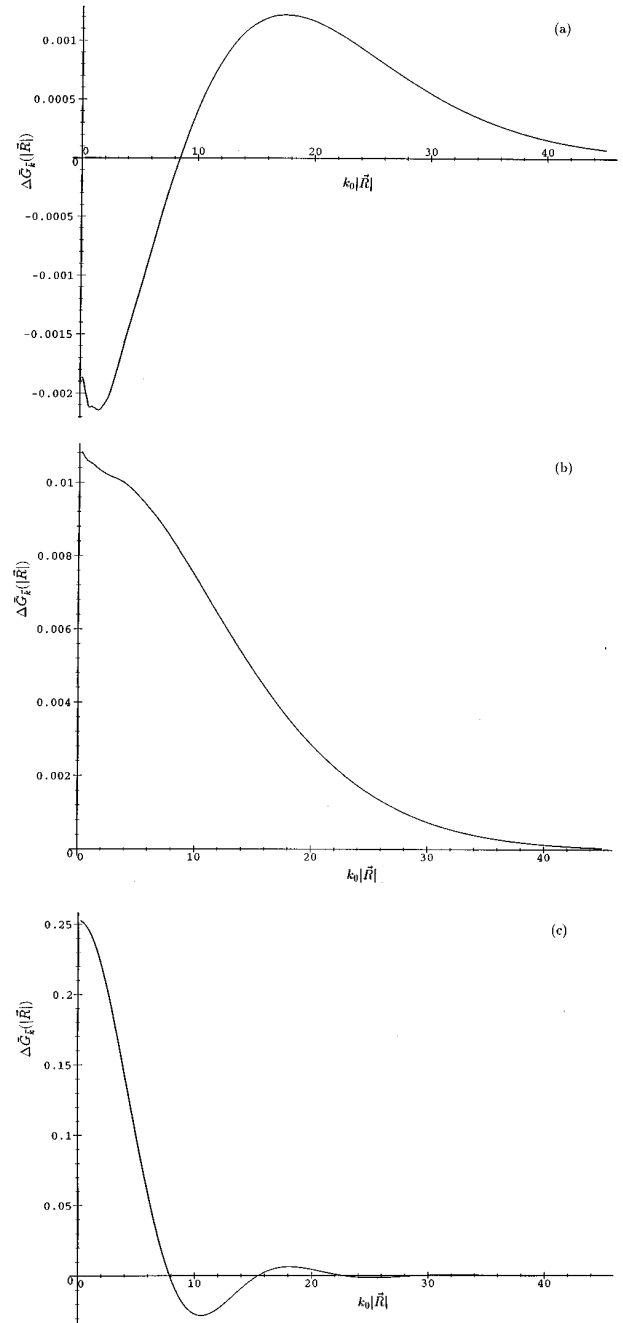
Fig. 2 Fourier transform of $i\Delta G_{\mathbf{k}}(\mathbf{Q})$, namely, $\Delta\bar{G}_{\mathbf{k}}(|\mathbf{R}|)$ $\equiv\int_{\mathbf{Q}}\exp[i\mathbf{Q}\cdot\mathbf{R}][i\Delta G_{\mathbf{k}}(\mathbf{Q})]$ for the case when: (a) $\mathbf{k}\cdot\mathbf{R}/|\mathbf{R}|=1.0k_0$; (b) $\mathbf{k}\cdot\mathbf{R}/|\mathbf{R}|=0.99k_0$; (c) $\mathbf{k}\cdot\mathbf{R}/|\mathbf{R}|=0.80k_0$. It was calculated for the model of identical polystyrene spheres in water with $\phi=0.1$ and $a=20k_0^{-1}$. Note that $\Delta\bar{G}_{\mathbf{k}}(|\mathbf{R}|)$ is real because from Eq. (20) we have $[\Delta G_{\mathbf{k}}(\mathbf{Q})]^+=-\Delta G_{\mathbf{k}}(-\mathbf{Q})$.

longer distance than the transport mean-free-path, is absent in radiative transfer theory. This is the most significant difference between the results of these two theories. (2) The values of parameters $\lambda_{\ell\ell'}^{[m]}$ and $D_{\ell\ell'}^{[m]}$ given by the radiative transfer theory for other remaining terms are, in general, not the same as those given by our wave theory except for the terms with ℓ or $\ell'=0$. When one of ℓ

and ℓ' is equal to zero, the radiative transfer theory also gives $\lambda_{\ell\ell'}^{[0]} = \infty$ (in the absence of absorption).

The above discussion shows that the conventional radiative transfer theory is an approximation to our wave theory, and the difference between these two theories remains important on scales longer than the transport mean-free-path. Nonlocal corrections to particlelike transport of photons appear even without consideration of the interference of different diffusion paths. These nonlocal corrections arise from the fact that wavelike coherence persists on long length scales in a medium with a nontrivial underlying structure. This would be absent in a "white noise" model consisting of spatially uncorrelated point scatterers. The diffusion model is insensitive to the important distinctions between white noise disorder and a scattering medium with specific cellular structures arranged in a specific order. An extreme illustration of this effect is that of a periodic dielectric microstructure. Here, wavelike coherence persists on an infinite length scale due to perfect coherent interference between different single scattering events, giving rise to a propagating Bloch wave. Biological tissue is an intermediate case in which this wave coherence may extend on scales that are large compared with the transport mean-free-path.

We mention finally that coherent backscattering effects[18,19] may be systematically incorporated into wave theory by replacing $\tilde{B}_h(\mathbf{k}-\mathbf{k}_1)$ in Eq. (19) by an "irreducible vertex function," $U_{\mathbf{k},\mathbf{k}_1}(\mathbf{Q})$.[16] This vertex function has a perturbation expansion in the small parameter $(\lambda/\ell^*)^2$. The leading term in this expansion is in fact $\tilde{B}_h(\mathbf{k}-\mathbf{k}_1)$. The $\mathbf{Q}$ dependence, obtained at a higher order in perturbation theory, gives rise to further nonlocality in the resulting radiative transfer equation.

4 MULTIPLE LIGHT SCATTERING NEAR AN INHOMOGENEITY

In Sec. 2 we described the relationship between the coherence propagator Γ_h and the underlying dielectric microstructure characterized by the translationally invariant function $B_h(\mathbf{r}-\mathbf{r}') \equiv \omega^4/c^4 \langle \epsilon_h^*(\mathbf{r}) \times \epsilon_h(\mathbf{r}') \rangle_{\text{ensemble}}$. In the presence of a localized inhomogeneity, the dielectric autocorrelation is no longer translationally invariant. This loss of translational symmetry is related to the function $V(\mathbf{R})$ which appears in Eq. (7) and which describes the fixed location and shape of the inhomogeneity. We consider, for simplicity, an inhomogeneous region that is located near some central point $\mathbf{R}_0$. The inhomogeneity may absorb light and may have different scattering characteristics than the homogeneous background. We assume that the internal correlations of the inhomogeneity, like the background, are isotropic after ensemble averaging. That is to say, $B_i(\mathbf{r}) = B_i(r)$ where $r \equiv |\mathbf{r}|$. It is useful to define the matrix

$$b_{\ell m,\ell'm'} \equiv \langle \psi_{\ell m}|B_i|\psi_{\ell'm'}\rangle. \tag{26}$$

From the isotropy assumption for $B_i(\mathbf{r})$, it follows that this matrix is diagonal. We define

$$b_{\ell m,\ell'm'} \equiv b_\ell \delta_{\ell\ell'} \delta_{mm'}. \tag{27}$$

This together with the fact that only the $n=0$ principal quantum number states contribute to Γ_h (weak scattering), leads to the result that the inhomogeneity does not mix the partial waves with different n or m indexes of the coherence propagator Γ_h. It is useful to introduce a $(\ell_{\max}-|m|) \times (\ell_{\max}-|m|)$ matrix $\hat{\Gamma}_h^{[m]}(\mathbf{R}-\mathbf{R}')$ whose (ℓ,ℓ')th element is defined by

$$(\hat{\Gamma}_h^{[m]}(\mathbf{R}-\mathbf{R}'))_{\ell\ell'} \equiv \frac{1}{4\pi D_{\ell\ell'}^{[m]}} \frac{\exp[-|\mathbf{R}-\mathbf{R}'|/\lambda_{\ell\ell'}^{[m]}]}{|\mathbf{R}-\mathbf{R}'|^{(1+|\ell-\ell'|)}}. \tag{28}$$

It follows from the above assumptions that the full coherence propagator (including the inhomogeneity) can be expressed in the form

$$\Gamma(\mathbf{R},\mathbf{R}';\mathbf{k},\mathbf{k}') = \sum_{m=-l_{\max}}^{\ell_{\max}} \sum_{\ell,\ell'=|m|}^{\ell_{\max}} \Gamma_{\ell\ell'}^{[m]}(\mathbf{R},\mathbf{R}')$$
$$\times \psi_{\ell m}^*(\mathbf{k}) \psi_{\ell'm}(\mathbf{k}'), \tag{29}$$

where $\Gamma_{\ell\ell'}^{[m]}(\mathbf{R},\mathbf{R}')$ is the (ℓ,ℓ')th element of a $(\ell_{\max}-|m|) \times (\ell_{\max}-|m|)$ matrix $\hat{\Gamma}^{[m]}(\mathbf{R},\mathbf{R}')$, which will be determined.

In the absence of the inhomogeneity [$V(\mathbf{R})=0$], $\hat{\Gamma}^{[m]}(\mathbf{R},\mathbf{R}')$ reduces to $\hat{\Gamma}_h^{[m]}(\mathbf{R}-\mathbf{R}')$. The presence of the inhomogeneity, however, removes the translational symmetry of the problem. Using the same set of approximations which were used in the derivation of Γ_h, namely the noninterference of different radiative transfer paths, it is straightforward to show[20] that $\hat{\Gamma}^{[m]}(\mathbf{R},\mathbf{R}')$ satisfies the following linear integral equation:

$$\hat{\Gamma}^{[m]}(\mathbf{R},\mathbf{R}') = \hat{\Gamma}_h^{[m]}(\mathbf{R}-\mathbf{R}') + \int_{\mathbf{R}''} \hat{\Gamma}_h^{[m]}(\mathbf{R}-\mathbf{R}'')$$
$$\times V(\mathbf{R}'')\hat{b}^{[m]}\hat{\Gamma}^{[m]}(\mathbf{R}'',\mathbf{R}'), \tag{30}$$

where $\hat{b}^{[m]}$ is a constant diagonal matrix whose ℓth diagonal element is b_ℓ, which describes the internal, ensemble-averaged microstructure of the inhomogeneity. For a spherical tumor of radius b, centered at $\mathbf{R}_0$, the "potential" V can be described by the function

$$V(\mathbf{R}) = \Theta(b-|\mathbf{R}-\mathbf{R}_0|), \tag{31}$$

where the step function is defined by $\Theta(x)=1$ for $x \geq 0$ and $\Theta(x)=0$ for $x<0$.

The integral equation (3) for the inhomogeneous propagator is remarkably similar to the Lippmann-Schwinger equation[14] describing the quantum mechanical scattering of a particle from a static potential well. For the quantum particle, $\hat{\Gamma}_h^{[m]}(\mathbf{R}-\mathbf{R}')$ in

Eq. (30) would be replaced by the free-particle propagator (3) and $V(\mathbf{R}'')$ would be replaced by the quantum mechanical scattering potential. The ensemble-averaged, multiple scattering problem differs from the conventional quantum scattering problem in two fundamental respects. First of all, Eq. (30) constitutes a set of $(\ell_{\max}-|m|)\times(\ell_{\max}-|m|)$ coupled equations. Second, the ''background'' propagators $\hat{\Gamma}_h^{[m]}$ are damped rather than purely oscillatory, since the higher order partial waves of the coherence function fail to propagate in the disordered medium on scales much, much greater than the transport mean-free-path ℓ^*. It is significant to note, however, that the damping length scales are as large as twenty times the transport mean-free-path in some of the models we have studied. Finally, we mention that in the case of strong scattering by the homogeneous background (violating the fact that only the $n=0$ principle quantum number states contribute to Γ_h) or in the case of anisotropic internal correlations within the inhomogeneity $[B_i(\mathbf{r})\neq B_i(r)]$, the matrix $b_{n\ell m,n'\ell'm'}$ [generalization of Eq. (26)] has off-diagonal elements. This leads to a coupling between the partial wave propagators in Eq. (30) for different values of m and n.

The solution of the coupled system of integral equations is similar in structure to the solution of the Lippmann-Schwinger equation in quantum mechanics. We consider the asymptotic behavior of Eq. (30) when the source and detectors are far from the inhomogeneity ($|\mathbf{R}-\mathbf{R}_0|\gg b$ and $|\mathbf{R}'-\mathbf{R}_0\gg b$). For this purpose, we rewrite Eq. (30) as follows:

$$\hat{\Gamma}^{[m]}(\mathbf{R},\mathbf{R}')$$
$$= \hat{\Gamma}_h^{[m]}(\mathbf{R}-\mathbf{R}') + \int_{\mathbf{R}''}\hat{\Gamma}_h^{[m]}(\mathbf{R}-\mathbf{R}'')$$
$$\times V(\mathbf{R}'')\hat{b}^{[m]}\hat{\Gamma}_h^{[m]}(\mathbf{R}''-\mathbf{R}')$$
$$+ \int_{\mathbf{R}''\mathbf{R}'''}\hat{\Gamma}_h^{[m]}(\mathbf{R}-\mathbf{R}'')V(\mathbf{R}'')\hat{b}^{[m]}\hat{\Gamma}^{[m]}(\mathbf{R}'',\mathbf{R}''')$$
$$\times V(\mathbf{R}''')\hat{b}^{[m]}\hat{\Gamma}_h^{[m]}(\mathbf{R}'''-\mathbf{R}'). \quad (32)$$

In the limit $|\mathbf{R}-\mathbf{R}_0|\gg b$, we may use the fact that $|\mathbf{R}''-\mathbf{R}_0|\ll|\mathbf{R}-\mathbf{R}_0|$ to rewrite $|\mathbf{R}-\mathbf{R}''|=|\mathbf{R}-\mathbf{R}_0-(\mathbf{R}''-\mathbf{R}_0)|$ in (32), and then Taylor expand this expression in the small parameter $|\mathbf{R}''-\mathbf{R}_0|$. Similar expansion also applies to the limit $|\mathbf{R}'-\mathbf{R}_0|\gg b$.

These expansions yield the asymptotic behavior of the partial-wave coherence propagator when both source and detector are far from the inhomogeneity:

$$\Gamma_{\ell\ell'}^{[m]}(\mathbf{R},\mathbf{R}')$$
$$\simeq \frac{1}{4\pi D_{\ell\ell'}^{[m]}}\frac{\exp[-|\mathbf{R}-\mathbf{R}'|/\lambda_{\ell\ell'}^{[m]}]}{|\mathbf{R}-\mathbf{R}'|^{1+|\ell-\ell'|}}$$

$$+ \sum_{i,j=|m|}^{\ell_{\max}}f_{\ell\ell',ij}^{[m]}(\theta,i/\lambda_{\ell i}^{[m]},i/\lambda_{j\ell'}^{[m]})$$
$$\times \frac{\exp[-|\mathbf{R}-\mathbf{R}_0|/\lambda_{\ell i}^{[m]}-|\mathbf{R}'-\mathbf{R}_0|/\lambda_{j\ell'}^{[m]}]}{4\pi D_{\ell i}^{[m]}D_{j\ell'}^{[m]}|\mathbf{R}-\mathbf{R}_0|^{1+|\ell-i|}|\mathbf{R}'-\mathbf{R}_0|^{1+|\ell'-j|}}.$$
$$(33)$$

Here, $\cos\theta\equiv(\mathbf{R}_0-\mathbf{R}')\cdot(\mathbf{R}-\mathbf{R}_0)/(|\mathbf{R}_0-\mathbf{R}'\|\mathbf{R}-\mathbf{R}_0|)$ describes the angle between the line connecting the source to inhomogeneity and the line connecting the inhomogeneity to the detector. The function $f_{\ell\ell',ij}^{[m]}(\theta,i/\lambda_{\ell i}^{[m]},i/\lambda_{j\ell'}^{[m]})$ is the analog of a scattering amplitude in quantum mechanics. A straightforward calculation leads to the following formal expression for this scattering amplitude:

$$f_{\ell\ell',ij}^{[m]}(\theta,i/\lambda_{\ell i}^{[m]},i/\lambda_{j\ell'}^{[m]}) = \frac{1}{4\pi}\int_{\boldsymbol{\rho}''}\exp[\boldsymbol{\rho}''\cdot\hat{R}/\lambda_{\ell i}^{[m]}]$$
$$\times V(\mathbf{R}_0+\boldsymbol{\rho}'')[\hat{b}^{[m]}$$
$$\times \hat{\Psi}^{(m,\ell')}(\mathbf{R}_0+\boldsymbol{\rho}'')]_{ij},$$
$$(34)$$

where $\hat{R}\equiv(\mathbf{R}-\mathbf{R}_0)/|\mathbf{R}-\mathbf{R}_0|$ and the ''scattering wave function'' satisfies the matrix integral equation:

$$\hat{\Psi}^{(m,\ell')}(\mathbf{R}) = \hat{E}^{(m,\ell')}(z) + \int_{\mathbf{R}''}\hat{\Gamma}_h^{[m]}(\mathbf{R}-\mathbf{R}'')$$
$$\times V(\mathbf{R}'')\hat{b}^{[m]}\hat{\Psi}^{(m,\ell')}(\mathbf{R}''). \quad (35)$$

Here, $z\equiv(\mathbf{R}'-\mathbf{R}_0)\cdot(\mathbf{R}-\mathbf{R}_0)/|\mathbf{R}'-\mathbf{R}_0|$, and $[\hat{E}^{(m,\ell')}\times(z)]_{ij} = \exp[z/\lambda_{j\ell'}^{[m]}\delta_{ij}]$. Equation (35) is a matrix type of Lippmann-Schwinger equation analytically continued to imaginary wave vectors $i/\lambda_{\ell\ell'}^{[m]}$.

The above analysis demonstrates the formal relationship between scattering from a statistical inhomogeneity in a homogeneous multiple-scattering background and a quantum mechanical type of scattering governed by Eq. (35). The measurement of the scattering amplitude $f_{\ell\ell',ij}^{[m]}(\theta,i/\lambda_{\ell i}^{[m]},i/\lambda_{j\ell'}^{[m]})$ coupled with knowledge of the parameters $\lambda_{\ell\ell'}^{[m]}$, and $D_{\ell\ell'}^{[m]}$, (from measurement of transport in the homogeneous background) leads to a complete characterization of the inhomogeneity (tumor). The scattering amplitude in this illustration may be measured by using a coherent light source at one spot on the sample surface and then performing phase-space tomography at a large number of other spots along the sample surface. Reconstruction of the Wigner coherence function at any given spot requires a large number of intensity measurements at the spot. A second level of reconstruction consists of evaluating $V(\mathbf{R})$ and $B_i(\mathbf{r})$ from comparison of the reconstructed Wigner function between a large number of different spots along the sample surface. Reconstruction of the tumor profile $V(\mathbf{R})$

and the tumor's internal characteristic function $B_i(\mathbf{r})$ reduces to a quantum inverse scattering problem.[21]

5 DISCUSSION

We have outlined a formal analogy between wave propagation in a multiple scattering medium with a statistical inhomogeneity and the quantum mechanical scattering of a particle by a localized potential. Our multiple scattering theory is more fundamental than conventional radiative transfer theory in which photons are treated as classical particles. In this analogy, the disorder-averaged coherence function $\langle E^*(\mathbf{r}_1)E(\mathbf{r}_2)\rangle_{\text{ensemble}}$ plays the role of a scattering wave function. The coordinate $\mathbf{R}\equiv(\mathbf{r}_1+\mathbf{r}_2)/2$ corresponds to the center of mass of the quantum particle and the relative coordinate $\mathbf{r}\equiv\mathbf{r}_1-\mathbf{r}_2$ corresponds to some internal degree of freedom of the quantum particle. By taking the Fourier transform of the coherence function with respect to $\mathbf{r}$, we obtain the Wigner function $I(\mathbf{R},\mathbf{k})$. This function is the wave analog of the specific light intensity that is used in a Boltzmann-type transport theory. Alternatively, the spectral content of the radiation field at $\mathbf{R}$ may be described in terms of a set of "eigenfunctions" $\Psi_{\ell m}(\mathbf{k})$. The precise form of these eigenfunctions is determined by the homogeneous dielectric autocorrelation function $B_h(\mathbf{r})\equiv\omega^4/c^4\langle\epsilon_h^*(\mathbf{r})\epsilon_h(0)\rangle_{\text{ensemble}}$. In particular $\psi_{\ell m}(\mathbf{k})$ are the Fourier transforms of the bound-state wave functions in the "potential" $-B_h(\mathbf{r})$. If the initial mode at point $\mathbf{R}'$ is $\psi_{\ell m}(\mathbf{k})$, then, as the radiation propagates from point $\mathbf{R}'$ to $\mathbf{R}$, the intensity remaining in the initial mode $\psi_{\ell m}(\mathbf{k})$ decreases by the factor $\exp[-|\mathbf{R}-\mathbf{R}'|/\lambda_{\ell\ell}^{[m]}]/(4\pi D_{\ell\ell}^{[m]}|\mathbf{R}-\mathbf{R}'|)$. In many cases of physical importance, the coherence length λ_{11}^0 may exceed the transport mean-free-path by an order of magnitude. The parameters $\lambda_{\ell\ell}^{[m]}$ and $D_{\ell\ell}^{[m]}$ are related to the "energy eigenvalues" of the potential $-B_h(\mathbf{r})$. Here, $\lambda_{00}^{[0]}=\infty$ and $D_{00}^{[0]}$ is the optical diffusion coefficient. In the quantum mechanical analogy, $B_h(\mathbf{r})$ plays the role of an internal binding potential for the (composite) particle and the $\psi_{\ell m}$ are the ground and excited states of the particle. Depending on the nature of the coherent light source, some superposition of the ground (diffusion mode) and excited states may be created. As the particle propagates from point $\mathbf{R}'$ to $\mathbf{R}$, the higher excited states are damped and the internal state of the particle relaxes to the ground state.

In the presence of a statistical inhomogeneity, $V(\mathbf{R})B_i(\mathbf{r})$, the center of mass of the composite particle experiences an external potential proportional to $V(\mathbf{R})$. When the internal state of the particle is given by $\psi_{\ell m}$, the external potential from which the particle scatters is given by $\langle\psi_{\ell m}|B_i|\psi_{\ell m}\rangle V(\mathbf{R})$.

The above analogy and the mathematical formalism associated with it opens the possibility of high-resolution multiple light scattering tomography. The propagation of the total intensity field $\langle|E(\mathbf{r})|^2\rangle_{\text{ensemble}}$ probes the nature of the dielectric medium on scales that are large compared with the transport mean-free-path ℓ^*. The internal structure of the coherence function $\langle E^*(\mathbf{r}_1)E(\mathbf{r}_2)\rangle_{\text{ensemble}}$ probes the structure of the dielectric medium on scales ranging from ℓ^* down to the optical wavelength. These considerations clearly underscore the enhanced sensitivity and resolving power of coherent multiple light scattering tomography beyond that allowed by the diffusion model.

APPENDIX: RELATIONSHIP OF THE WIGNER DISTRIBUTION FUNCTION TO THE SPECIFIC LIGHT INTENSITY

The Wigner distribution function, $I(\mathbf{R},\mathbf{k})$, defined in Eq. (1) as the electric field mutual coherence function is not positive definite. This differs from the specific light intensity, $I^c(\mathbf{R},\mathbf{k})$, of conventional radiative transfer theory, defined by Eq. (21). The specific intensity is a measure of the number of photons in a vicinity of the point $\mathbf{R}$ travelling in the direction of the wave vector $\mathbf{k}$ and is by definition positive definite. As a consequence of the wave nature of the photon, the specific intensity $I^c(\mathbf{R},\mathbf{k})$, refers to coarse-grained regions in coordinate space $\mathbf{R}$ and momentum space $\mathbf{k}$, such that the fundamental uncertainty relation $\Delta R_i\Delta k_i\geqslant 1$, $i=x,y,z$. We demonstrate briefly in the following paragraphs that a suitable coarse graining of the Wigner distribution leads to a positive definite distribution which we identify with the specific light intensity. More details on the subject of coarse graining of the Wigner function can be found in Refs. 22 and 23.

Consider the coarse-graining function

$$\rho(\mathbf{R},\mathbf{k};\mathbf{R}',\mathbf{k}')\equiv\frac{1}{\pi^3}\exp[-(\mathbf{R}'-\mathbf{R})^2/(\Delta R)^2]$$

$$\times\exp[-(\mathbf{k}'-\mathbf{k})^2/(\Delta k)^2] \quad (36a)$$

with the constraint that

$$\Delta R\Delta k=1. \quad (36b)$$

It is straightforward to verify that

$$\int d^3\mathbf{R}d^3\mathbf{k}\rho(\mathbf{R},\mathbf{k};\mathbf{R}',\mathbf{k}')=(\Delta R\Delta k)^3=1. \quad (37)$$

Applying this coarse-graining operation to the Wigner distribution, we obtain

$$I^c(\mathbf{R},\mathbf{k}) = \int d^3\mathbf{R}'d^3\mathbf{k}'\rho(\mathbf{R},\mathbf{k};\mathbf{R}',\mathbf{k}')I(\mathbf{R}',\mathbf{k}')$$

$$= \frac{1}{\pi^3}\int d^3\mathbf{R}d^3\mathbf{r}d^3\mathbf{k}'\rho(\mathbf{R},\mathbf{k};\mathbf{R}',\mathbf{k}')$$

$$\times\exp[-i\mathbf{k}'\cdot\mathbf{r}]\langle E^*(\mathbf{R}'+\mathbf{r}/2)$$

$$\times E(\mathbf{R}'-\mathbf{r}/2)\rangle_{\text{ensemble}}. \tag{38}$$

Using the definition of the coarse-graining function (36) and making the change of variables $\mathbf{u}=\mathbf{R}'+\mathbf{r}/2$ and $\mathbf{v}=\mathbf{R}'-\mathbf{r}/2$, we may integrate (38) with respect to $\mathbf{k}'$ to obtain:

$$I^c(\mathbf{R},\mathbf{k}) = \left[\frac{(\Delta k)^2}{\pi}\right]^{3/2}\int d^3\mathbf{u}d^3\mathbf{v}\langle E^*(\mathbf{u})E(\mathbf{v})\rangle_{\text{ensemble}}$$

$$\times\exp[-i\mathbf{k}\cdot(\mathbf{u}-\mathbf{v})]$$

$$\times\exp\left[-\frac{(\Delta k)^2}{4}(\mathbf{u}-\mathbf{v})^2 - \frac{(\mathbf{u}+\mathbf{v}-2\mathbf{R})^2}{4(\Delta R)^2}\right]. \tag{39}$$

Using the fact that $(\Delta k)^2 = 1/(\Delta R)^2$, it follows that

$$I^c(\mathbf{R},\mathbf{k}) = \frac{1}{\pi^{3/2}(\Delta R)^3}\int d^3\mathbf{u}d^3\mathbf{v}\langle E^*(\mathbf{u})E(\mathbf{v})\rangle_{\text{ensemble}}$$

$$\times\exp[-i\mathbf{k}\cdot(\mathbf{u}-\mathbf{v})]$$

$$\times\exp\left[-\frac{(\mathbf{u}-\mathbf{R})^2+(\mathbf{v}-\mathbf{R})^2}{2(\Delta R)^2}\right]$$

$$= \frac{1}{\pi^{3/2}(\Delta R)^3}\left\langle\left|\int d^3\mathbf{u}E(\mathbf{u})\exp[-i\mathbf{k}\cdot\mathbf{u}\right.\right.$$

$$\left.\left.-(\mathbf{u}-\mathbf{R})^2/[2(\Delta R)^2]]\right|^2\right\rangle_{\text{ensemble}},$$

which is indeed positive definite. We identify this coarse-grained version of the Wigner distribution function with the specific light intensity of conventional radiative transfer theory.

Acknowledgments

REFERENCES

1. B. Chance, ''Optical method'' *Ann. Rev. Biophys. Biophys. Chem.* **20**, 1 (1991).
2. D. Huang et al., ''Optical coherence tomography'' *Science* **254**, 1178 (1991).
3. D. Delpy, ''Optical spectroscopy for diagnosis,'' *Physics World* **7**, 34 (1994).
4. D. A. Benaron and D. K. Stevenson, ''Optical time-of-flight and absorbance imaging of biological media,'' *Science* **259**, 1463 (1993).
5. A. Yodh and B. Chance, ''Spectroscopy and imaging with diffusing light,'' *Physics Today* **48**, 34 (1995).
6. L. Wang, P. P. Ho, C. Liu, G. Zhang, and R. R. Alfano, ''Ballistic 2-D imaging through scattering walls using an ultrafast optical Kerr gate,'' *Science* **253**, 769 (1991).
7. J. Fishkin and E. Gratton, ''Propagation of photon-density waves in strongly scattering media containing an absorbing semi-infinite plane bounded by a straight edge,'' *J. Opt. Soc. Am.* **A10**, 127 (1993).
8. S. R. Arridge et al., ''Performance of an iterative reconstructive algorithm for near infrared absorption and scattering imaging,'' *Proc. SPIE* **1888**, 360 (1993).
9. D. R. Wyman, M. S. Patterson, and B. C. Wilson, ''Similarity relations for the interaction parameters in radiation transport,'' *Appl. Opt.* **28**, 5243 (1989).
10. K. M. Case and P. F. Zweifel, *Linear Transport Theory*, Addison-Wesley, Reading, MA (1976).
11. D. F. McAlister, M. Beck, L. Clarke, A. Mayer, and M. G. Raymer, ''Optical phase retrieval by phase-space tomography and fractional-order Fourier transforms,'' *Opt. Lett.* **20**, 1181 (1995).
12. M. Hillery, R. F. O'Connel, M. O. Scully and E. P. Wigner, ''Distribution functions in physics: Fundamentals,'' *Physics Reports* **106**, 121 (1984).
13. M. G. Raymer, M. Beck, and D. F. McAlister, ''Complex wave field reconstruction using phase-space tomography,'' *Phys. Rev. Lett.* **72**, 1137 (1994).
14. K. Gottfried, *Quantum Mechanics: Fundamentals Vol. 1*, Chapter III, Benjamin/Cummings, Reading, MA (1966).
15. S. John and M. J. Stephen, ''Wave propagation and localization in a long-range-correlated random potential,'' *Phys. Rev.* **B28**, 6358 (1983).
16. F. C. MacKintosh and S. John, ''Diffusing-wave spectroscopy and multiple scattering of light in correlated random media,'' *Phys. Rev.* **B40**, 2383 (1989).
17. W. Hess and R. Klein, ''Generalized hydrodynamics of systems of Brownian particles,'' *Adv. Phys.* **32**, 173 (1983).
18. M. P. van Albada and A. Lagendijk, ''Observation of weak localization of light in a random medium,'' *Phys. Rev. Lett.* **55**, 2692 (1985).
19. P. E. Wolf and G. Maret, ''Weak localization and coherent backscattering of photons in disordered media,'' *Phys. Rev. Lett.* **55**, 2696 (1985).
20. S. John, G. Pang, and Y. Yang, submitted to *Phys. Rev. E.*
21. K. Chadan and P. C. Sabatier, *Inverse Problems in Quantum Scattering Theory,* 2nd ed., Springer-Verlag, New York (1989).
22. N. D. Cartwright, ''A Non-negative Wigner-type distribution,'' *Physica* **83A**, 210 (1976).
23. K. Takahashi, ''Wigner and Husimi functions in quantum mechanics,'' *J. Phys. Soc. Jpn.* **55**, 762 (1986).